

Ageing of Lanthanum Strontium Copper Orthoferrite Powders for Sensing Layers

Jean-Marc Tulliani^a, Marta Maria Natile^b, Luca Tortora^{c,d}, Isabella Natali Sora^{*,e}

^aINSTM R.U. Politecnico di Torino, DISAT, Corso Duca degli Abruzzi 24, 10129 Torino, Italy

^bCNR-IENI, INSTM, Dipartimento di Scienze Chimiche, Università di Padova, Via F. Marzolo 1, 35131 Padova, Italy

^cUniversità di Roma "Roma Tre", Laboratorio di Analisi delle Superfici, Dipartimento di Fisica "E. Amaldi" and INFN, Via della Vasca Navale 84, 00146 Roma, Italy

^dUniversità di Roma "Tor Vergata", Dipartimento di Ingegneria Industriale, Via del Politecnico 1, 00133 Roma, Italy

^eINSTM R.U. Bergamo and Università di Bergamo, Dipartimento di Ingegneria e Scienze Applicate, Viale Marconi 5, 24044 Dalmine Italy

isabella.natali-sora@unibg.it

Nanosized powders of lanthanum strontium copper orthoferrites $\text{La}_{0.8}\text{Sr}_{0.2}\text{Fe}_{1-x}\text{Cu}_x\text{O}_{3-w}$ (LSFC) have been recently proposed as sensing component in chemical sensors for humidity detection. The LSFC powders were prepared by citrate auto-combustion of dry gel obtained from a solution of corresponding nitrates in a citric acid solution. The aged powders were investigated by chemical and structural analysis using X-ray Photoelectron Spectroscopy (XPS), Infrared Spectroscopy and X-Ray Powder Diffraction as a total loss of their sensing properties has been observed after about one year storage of the sensors at room temperature in the laboratory. The detection of surface hydroxides and carbonates species as well as very large Sr and Cu excess within the surface area were important results.

1. Introduction

The performance of semiconducting sensing layer gas sensors is correlated to their microstructural and electronic properties. Elemental substitution, surface states and grain size play an important role in the response of the material to gas. Recently, substituted LaFeO_3 semiconducting materials have been proposed as promising sensing layers in chemical sensors for humidity detection (Wang et al., 2005). Among them, the most widely studied series is characterized by the general formula $\text{La}_{1-x}\text{Sr}_x\text{Fe}_{1-y}\text{M}_y\text{O}_{3\pm w}$ (where M is usually a transition metal). In general, the partial substitution of La with divalent Sr influences the physical properties mainly through steric effects, whereas the partial substitution of Fe with a transition metal influences the electronic ground state properties. In $\text{La}_{0.8}\text{Sr}_{0.2}\text{Fe}_{1-x}\text{Cu}_x\text{O}_{3-w}$ (LSFC), the structural distortion from the ideal cubic perovskite AMO_3 can be attributed mostly to Fe/CuO₆ octahedron tilting and octahedral distortion. The second distortion mechanism is driven by the Jahn-Teller effect of the Cu ions. In particular doping with 10 mol % of Cu increases the octahedral distortion, moving towards a configuration with four longer and two shorter bond lengths (Sora et al, 2012).

With respect to the compound $\text{La}_{0.8}\text{Sr}_{0.2}\text{FeO}_{3-w}$ the presence of copper inside the orthoferrite structure causes a huge shift of the sensor response to low relative humidity (RH) values. As reported by Cavalieri et al. (2012) $\text{La}_{0.8}\text{Sr}_{0.2}\text{Fe}_{0.9}\text{Cu}_{0.1}\text{O}_{3-w}$ (LSFC10) shows a detection limit of 15-30% RH compared to 65-70% RH for $\text{La}_{0.8}\text{Sr}_{0.2}\text{FeO}_{3-w}$ depending on the thermal treatment, 800 and 900°C, respectively. Although the LSFC-based humidity sensors showed several promising properties such as low detection limit and a good reproducibility between several measurements, they suffered a loss of sensitivity when ageing. In particular, Tulliani et al. (2013) observed that after 1 y of ambient storage, the sensing material LSFC05 (doped with 5 mol % of Cu) lost quite completely its sensitivity to humidity, however the sensing activity of the film was mostly re-activated after a thermal treatment at 900 °C, and the sensors response to low RH was also restored. The de-activation

mechanism has not been fully interpreted yet. The XPS measurements have shown the presence of hydroxides and carbonates species on the surface of LSFC05 powders (Tulliani et al., 2013). However, after calcination at 900 °C the amount of carbonates decreased, even so it was significant, and it was impossible to gain information about the chemical environment of Cu due to the low signal to background ratio. In order to study the de-activation and re-activation mechanism and to ascertain the role of each cationic species at the formation of metal carbonates, LSFC10 powders with double amount of Cu were investigated by means of X-rays powder diffraction, X-ray photoelectron spectroscopy and Fourier-transformed Infrared at different ageing time.

2. Experimental

2.1 Powder Synthesis

$\text{La}_{0.8}\text{Sr}_{0.2}\text{Fe}_{0.9}\text{Cu}_{0.1}\text{O}_{3-w}$ (LSFC10) were prepared by auto-combustion of dry gel obtained from a solution of the corresponding nitrates in citric acid solution. Analytical grade La_2O_3 , $\text{Fe}(\text{NO}_3)_3 \cdot 9\text{H}_2\text{O}$, $\text{Cu}(\text{NO}_3)_2 \cdot 2.5\text{H}_2\text{O}$ and $\text{Sr}(\text{NO}_3)_2$, citric acid ($\text{C}_6\text{H}_8\text{O}_7 \cdot \text{H}_2\text{O}$), nitric acid (HNO_3 , 65 %), and 30 % aqueous NH_3 were supplied by Sigma-Aldrich and used as starting materials. The details have been previously reported (Caronna et al., 2009). When the combustion was completed, the resulting powder was treated at 600 °C for 3 h in air in order to remove any organic residue. Subsequently, the powders were thermal treated at 980 °C for 3 h, which is about the temperature used in the preparation of the gas sensors. The chemical stability of LSFC10 at high temperature was excellent as demonstrated by XRD (Mancini et al., 2014) and by SIMS and EDX analyses (Zurlo et al., 2014).

2.2 Characterization

X-ray powder diffraction data of the starting materials were collected using a Bruker D8 diffractometer equipped with $\text{Cu K}\alpha_1$ radiation. The measurement was performed in Bragg-Brentano geometry, with 0.02° increment size and collection time of 1 s/step over the 2θ angular range $5-70^\circ$. The average crystallite size was calculated using commercial software (EVA DIFFRAC, 2009). Software uses a full pattern matching (FPM) of the XRD pattern using an empirical model for the peak shape. The fitting of the scan is done by pseudo-Voigt functions. At the end of the FPM model the software calculates the crystallite size by the corrected Scherrer's equation for the instrumental broadening. XPS spectra were recorded by using a Perkin-Elmer PHI 5600ci spectrometer with a standard $\text{Al K}\alpha$ source (1486.6 eV) working at 250 W. The working pressure was less than 7×10^{-7} Pa. Extended spectra (survey) were collected in the range 0 – 1350 eV (187.85 eV pass energy, 0.5 eV step, 0.025 s/step). Detailed spectra were recorded for the following regions: La 3d, Sr 3d, Fe 2p, Cu 2p, O 1s, and C 1s (23.5 eV pass energy, 0.1 eV step, 0.2 s/step). The reported binding energies (BEs, standard deviation ± 0.1 eV) were corrected for the charging effects by considering the adventitious C 1s line at 285.0 eV. The atomic percentage, after a Shirley type background subtraction (Shirley, 1972) was evaluated by using the PHI sensitivity factors (Moulder et al., 1992). The IR spectra were collected in a Bruker Tensor 27 spectrophotometer accumulating 50 scans at a resolution of 4 cm^{-1} for the measurements in transmittance mode.

3. Results and Discussion

3.1 XRD Analysis

The analysis of the XRD data indicated that the starting powders used in this study are single phase, the carbonate species were not detected by XRD, since they are formed mainly on the surface due to exposure to ambient carbon dioxide (Figure 1). The compound crystallized in the perovskite-like cell of LaFeO_3 (orthorhombic symmetry), lattice parameters were in agreement with literature data on these system (Natali Sora et al., 2012). The mean crystallite size of LSFC10 treated at 980 °C was 55 nm, calculated from XRD data using Scherrer equation. The crystallite size decreases as the Sr/Cu doping increases (Natali Sora et al., 2013a).

3.2 XPS Analysis

In order to examine the surface chemical state and composition XPS measurements (shown in Figures 2, 3 and 4) were performed. La 3d peak positions (BEs) and shape are characteristic of La^{3+} in the perovskite (Figure 2) (Natile et al., 2014). The thermal cycle does not significantly influence the La 3d peak shape and binding energies. The fitting procedure of Sr 3d peak of the aged powder (Figure 2) reveals two pairs of spin-orbit doublets which indicate that strontium exists in different chemical environments. The Sr $3d_{5/2}$ contribution around 132.2 eV is characteristic of Sr^{2+} in perovskite phase, the one around 133.7 eV is due Sr^{2+} in SrCO_3 (Natile et al., 2008). After the regeneration treatment at 900 °C the contribution at higher BEs increases,

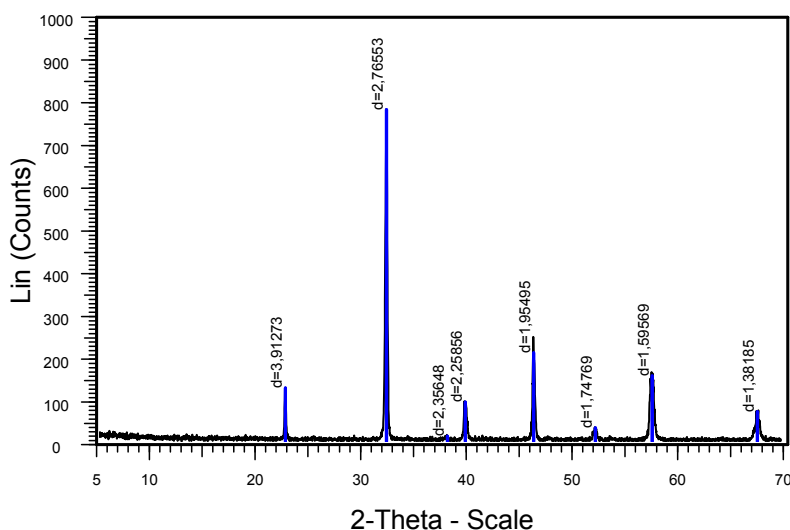


Figure 1: XRD patterns of the starting LSFC10 powders thermal treated at 980°C for 3 h.

suggesting an increase of carbonate species on the surface. Concerning Fe 2p core level (Figure 3) the peak shape and the BEs are characteristic of Fe³⁺ in perovskite (Natile et al., 2014). The Cu 2p peak positions (934.1 and 953.9 eV, respectively for Cu 2p_{3/2} and 2p_{1/2}) and the presence of shake-up contributions (around 942.6 and 962.7 eV) are consistent with how expected for Cu²⁺ in the perovskite structure (Glisenti et al., 2013) (Figure 3). The O 1s XP peak of aged powder (Figure 4) displays two different contributions corresponding to the perovskite lattice oxygen (at 528.9 eV) and other oxygen species that are present on the surface as hydroxyl groups and carbonates (around 531.6 eV) (Natile et al., 2014). After the regeneration it is evident a slight decrease of the contribution at higher BEs suggesting a lower surface contamination.

The nominal atomic ratio between Sr and La cations is 0.25. The XPS atomic composition reveals a large Sr segregation on the surface: Sr3d/La3d atomic ratio is 0.65 for the aged powder and increases up to 1.12 after a further thermal treatment at 900°C for 1 h, corresponding to the regeneration of the sensing layer reported in (Tulliani et al., 2013). This behaviour indicates that the surface Sr segregation is kinetically favoured at high temperature. The comparison between the Cu/Fe nominal atomic ratio (0.11) and Cu2p_{3/2}/Fe2p XPS atomic ratios (respectively 0.53 for aged powder and 0.40 after the regeneration treatment) reveals that copper has a greater tendency than the iron to segregate on the surface. Surface Sr segregation in perovskite materials has been extensively investigated, especially for application as cathode materials for solid oxide fuel cells (Jung et al., 2012).

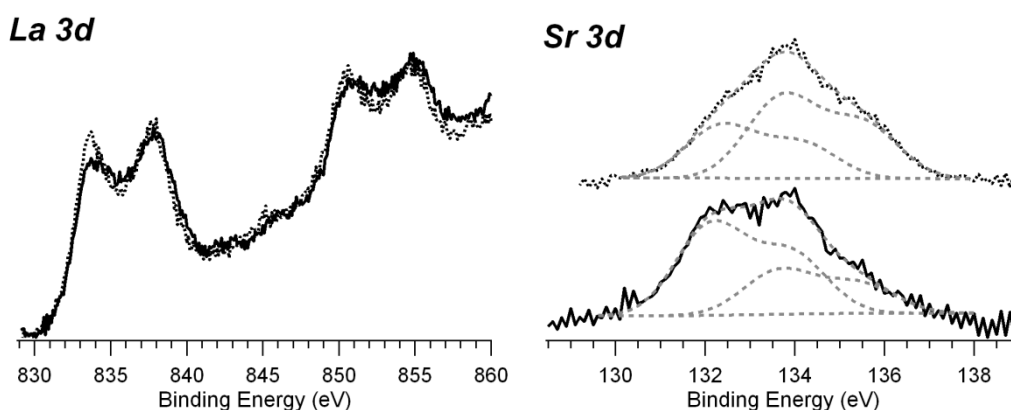


Figure 2: La 3d and Sr 3d XPS peaks obtained for LSFC10 sample aged 1 y (continuous line), and aged 1 y and then heated at 900 °C for 1 h (dotted line). Grey dashed lines refer to fitting. All spectra are normalized with respect to their maximum value.

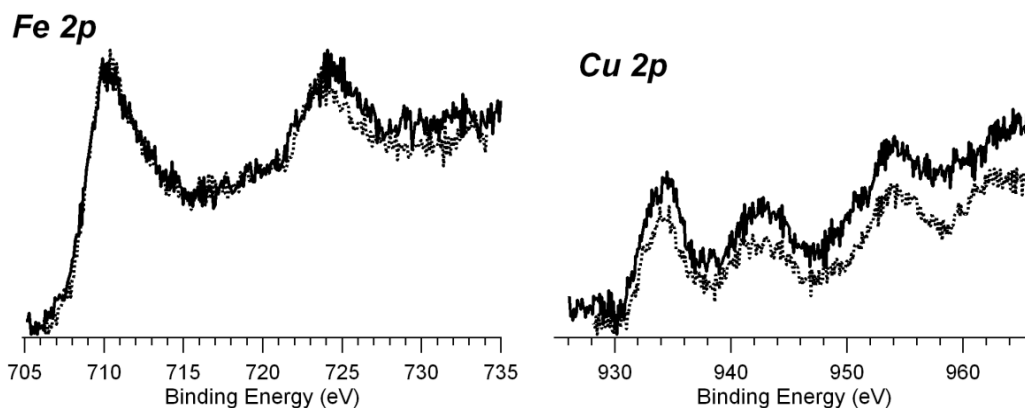


Figure 3: Fe 2p and Cu 2p XPS peaks obtained for LSFC10 sample aged 1 y (continuous line), and aged 1 y and then heated at 900 °C for 1 h (dotted line). All spectra are normalized with respect to their maximum value.

The most accepted explanation for Sr excess considers the lattice strain introduced in the structure of LaMO_3 (M is generally a transition metal) by the large Sr^{2+} cation when it partially substitutes La^{3+} cation ($\text{Sr}^{2+}(\text{XII}) = 1.44 \text{ \AA}$, $\text{La}^{3+}(\text{XII}) = 1.36 \text{ \AA}$). In the $\text{La}_{1-x}\text{Sr}_x\text{FeO}_3$ perovskite, Sr is under compressive stress which causes redistribution of the Sr cations within the (near) surface area. In the series $\text{La}_{0.8}\text{Sr}_{0.2}\text{Fe}_{1-y}\text{Cu}_y\text{O}_3$, the unit cell volume decreased with increasing Cu-doping (Natali Sora et al., 2012). Since Cu^{2+} cation is larger than the Fe^{3+} cation ($\text{Cu}^{2+}(\text{VI}) = 0.73 \text{ \AA}$, $\text{Fe}^{3+}(\text{VI}) = 0.645 \text{ \AA}$), the Cu atoms are under compressive stress. Moreover, Mössbauer measurements performed by Natali Sora et al. (2013b) on LSFC10 powders indicated the presence of two sextets with isomer shifts corresponding to Fe^{3+} , the presence of one sextet with isomer shift corresponding to Fe^{5+} and hyperfine parameters typical of Fe^{3+} and Fe^{5+} ions with octahedral coordination, while no structure related to Fe^{4+} is observed. The charge compensation mechanism (oxidation of Fe^{3+} cations to Fe^{5+}) further increases the compressive stress on the Cu atoms. As found for Sr segregation the source of the surface Cu segregation in Cu containing perovskites can be the mechanical strain gradient.

The IR spectrum of the LSFC10 powders after the thermal treatment at 900°C is shown in Figure 5. The broad band around 1,380-1,600 cm^{-1} associated with C-O stretching suggests the presence of a small amount of carbonate species. The thermal regeneration process decomposes the surface carbonate/hydroxide species, but a small amount was rapidly generated. The formation of carbonates, as a consequence of the interaction

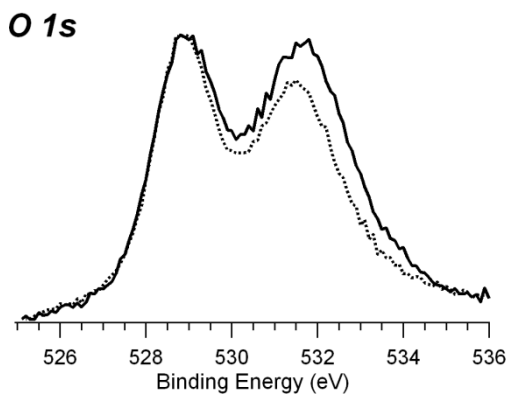


Figure 4: O 1s XPS peaks obtained for LSFC10 sample aged 1 y (continuous line), and aged 1 y and then heated at 900 °C for 1 h (dotted line). All spectra are normalized with respect to their maximum value.

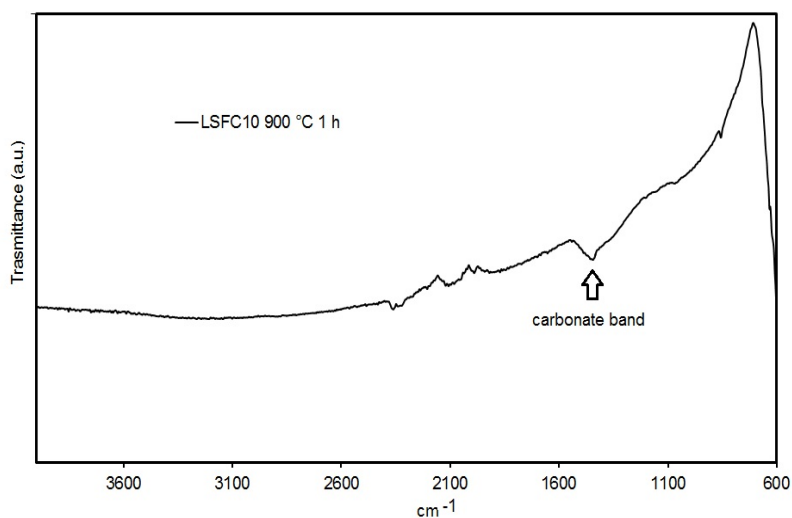


Figure 5: IR spectra obtained at room temperature for LSFC10 sample aged 1 y and then heated at 900 °C for 1 h.

with CO₂, can be attributed mostly to the structural properties of LSFC10. The ideal perovskite structure is cubic with the larger A site cations located at the corners of the cube, the B-site ions at the body centre, and the oxygen ions at the centres of the faces. The most important feature is that the oxide anion is coordinated by two relatively small and rather polarizing Fe/Cu cations, while they are only weakly polarized by the larger La/Sr cations (Figure 6). The average coordination of surface oxide ions is lowered to one, as a consequence they show strong nucleophilicity, which attacks the cation atom of CO₂ giving rise to stable surface carbonates (Daturi et al., 1995).

4. Conclusions

The XPS quantitative analysis of the aged LSFC10 powders indicated large surface Sr and Cu segregation, which can be caused by the mechanical strain gradient. The XPS atomic ratios were Sr/La = 0.65 and Cu/Fe =

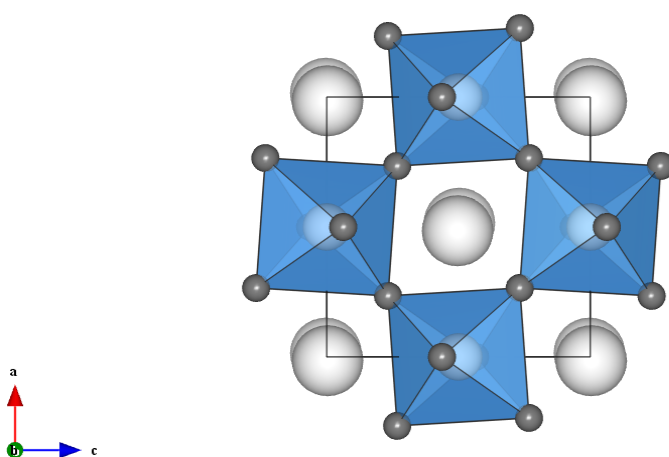


Figure 6: Projection along the b-axis of the orthorhombic crystal structure of $\text{La}_{0.8}\text{Sr}_{0.2}\text{Fe}_{0.9}\text{Cu}_{0.1}\text{O}_{3-w}$ showing the (Fe/Cu)O₆ octahedra, large circles represent La/Sr cations.

0.53, much higher than the nominal atomic ratios 0.25 and 0.11. At the same time the La and Fe cations diffused towards the bulk. The O 1s XP peak of aged powder displays two different contributions corresponding to the perovskite lattice oxygen and other oxygen species that are present on the surface as hydroxyl groups and carbonates. The second contribution slightly decreases after the regeneration treatment at 900 °C. The regeneration does not significantly influence the peak shape and binding energies of La 3d, Fe 2p and Cu 2p. On the contrary, after the thermal cycle at 900 °C the contribution at 133.7 eV, due to Sr²⁺ in SrCO₃, becomes more intense, suggesting an increase of carbonate species on the surface. Moreover, the XPS atomic ratio Sr/La after the thermal cycle is 1.12. This behaviour indicates that the surface Sr segregation was kinetically favored at high temperature. The Cu content was always in excess although after the thermal treatment the atomic ratio Cu/Fe was reduced to 0.40. The IR measurements showed that the regeneration treatment at 900 °C for 1 h decreased surface carbonates species, but a small amount was still present.

Acknowledgements

The financial support and collaboration of INSTM and of the Lombardy Region (Project "Ferriti di lantanio per nuove Fonti di Energia", Ferriti-NFE) is gratefully acknowledged. Laboratorio di Analisi delle Superfici gratefully acknowledges financial support from Fondazione Roma.

References

- Caronna T., Fontana F., Natali Sora I., Pelosato R., 2009, Chemical synthesis and structural characterization of the substitution compound LaFe_{1-x}Cu_xO₃ (x = 0-0.40), *Mat. Chem. Phys.* 116, 645-648
- Cavaliere A., Caronna T., Natali Sora I., Tulliani J.M., 2012, Electrical characterization of room temperature humidity sensors in La_{0.8}Sr_{0.2}Fe_{1-x}Cu_xO₃ (x = 0, 0.05, 0.10), *Ceram. Int.* 38, 2865-2872
- Daturi M., Busca G., Willey R.J., 1995, Surface and structure characterization of some perovskite-type powders to be used as combustion catalysis, *Chem. Mater.* 7, 2115-2126
- EVA Software, DIFFRACplus Release 2009, Bruker AXS
- Glisenti, A., Galenda, A., Natile, M. M., 2013, Steam reforming and oxidative steam reforming of methanol and ethanol: The behaviour of LaCo_{0.7}Cu_{0.3}O₃, *Appl. Catal. A* 453, 102-112
- Jung W.C., Tuller H.L., 2012, Investigation of surface Sr segregation in model thin film solid oxide fuel cell perovskite electrodes, *Energy Environ. Sci.* 5, 5370-5378
- Mancini A., Felice V., Natali Sora I., Malavasi L., Tealdi C., 2014, Chemical compatibility study of melilite-type gallate solid electrolyte with different cathode materials, *J. Solid State Chem.* 213, 287-292
- Moulder, J.F., Stickle, W.F., Sobol, P.E., Bomben, K.D., 1992, In *Handbook of X-ray Photoelectron Spectroscopy*; Chastain, J., Ed.; Physical Electronics: Eden Prairie, MN
- Natali Sora I., Caronna T., Fontana F., Fernandez C.D., Caneschi A., Green M., 2012, Crystal structures and magnetic properties of strontium and copper doped lanthanum ferrites, *J. Solid State Chem.* 191, 33-39
- Natali Sora I., Fontana F., Passalacqua R., Ampelli C., Perathoner S., Centi G., Parrino F., Palmisano L., 2013a, Photoelectrochemical properties of doped lanthanum orthoferrites, *Electrochimica Acta* 109, 710-715
- Natali Sora I., Caronna T., Fontana F., De Julián Fernández C., Caneschi A., Green M., Bonville P., 2013b, Charge compensation and magnetic properties in Sr and Cu doped La-Fe perovskites, *EPJ Web of Conferences* 40, 15005
- Natile M. M., Poletto F., Galenda A., Glisenti A., Montini T., De Rogatis L., Fornasiero P., 2008, La_{0.6}Sr_{0.4}Co_{1-y}Fe_yO_{3-δ} Perovskites: Influence of the Co/Fe Atomic Ratio on Properties and Catalytic Activity toward Alcohol Steam-Reforming, *Chem. Mater.* 20, 2314-2327
- Natile M. M., Ponzoni A., Concina I., Glisenti A., 2014, Chemical Tuning versus Microstructure Features in Solid-State Gas Sensors: LaFe_{1-x}Ga_xO₃, a Case Study, *Chem. Mater.* 26, 1505-1513
- Shirley D.A., 1972, High-Resolution X-Ray Photoemission Spectrum of the Valence Bands of Gold, *Phys. Rev. B* 5, 4709-4714.
- Tulliani J.M., Borgna M., Grigioni I., Sora I.N., 2013, Microstructural study of aged ferrite powders for sensing layers, *Ceram. Int.* 39, 4923-4927
- Wang J., Wu F., Song G., Wu N., Wang J., 2005, Complex Impedance Property of Humidity Sensing Material Lanthanum Orthoferrite, *Ferroelectrics* 323, 71-76
- Zurlo F., Di Bartolomeo E., D'Epifanio A., Felice V., Natali Sora I., Tortora L., Licoccia S., 2014, La_{0.8}Sr_{0.2}Fe_{0.8}Cu_{0.2}O_{3-δ} as "cobalt free" cathode for La_{0.8}Sr_{0.2}Ga_{0.8}Mg_{0.2}O_{3-δ} electrolyte, *J. Power Sources* 271, 187-194